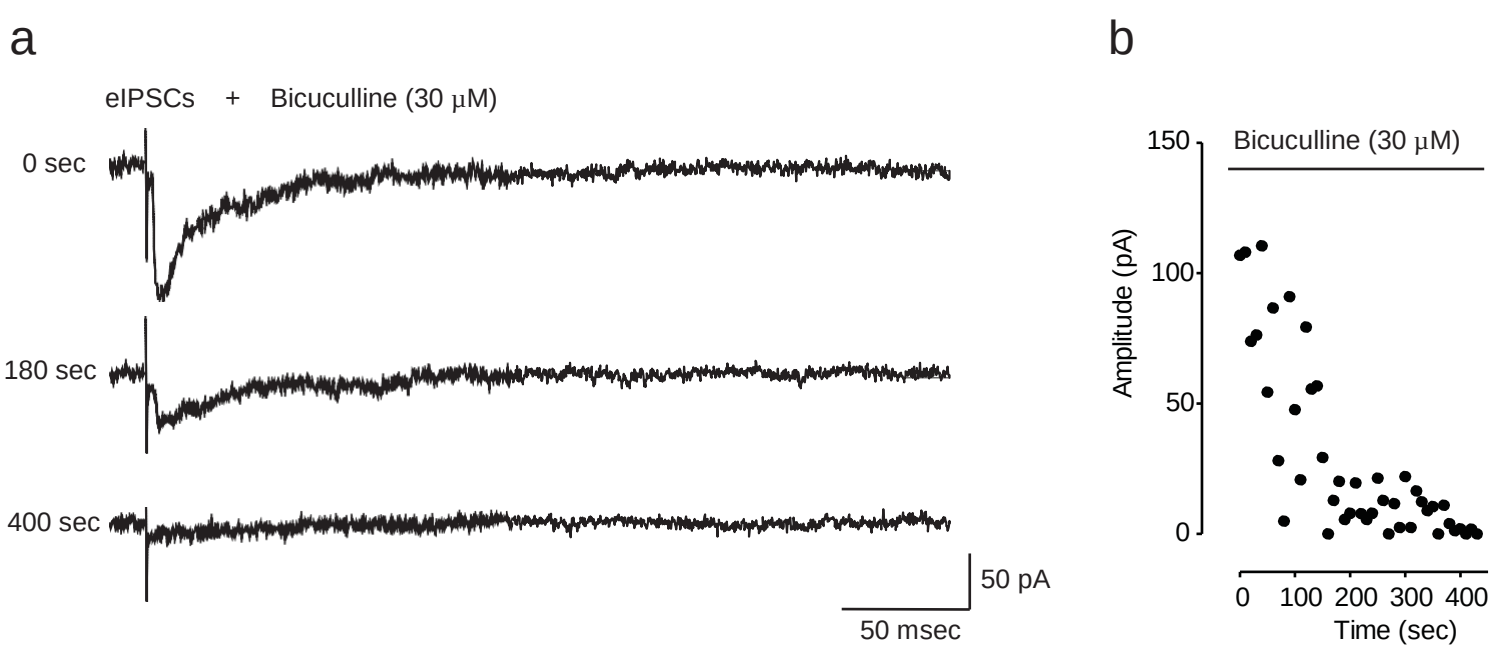

Supplementary Figure S1. Characterization of the inhibitory response evoked by stimulation of the medial perforant path.

a. Example of an inhibitory response obtained in a WT granule neuron upon stimulation of the medial perforant path. The evoked inhibitory response (eIPSC) is recorded in the presence of 50 µM D-APV, 10 µM CNQX and 5 µM CGP 55845. **b.** After addition of the $GABA_A$-receptor blocker bicuculline (30 µM) to the perfusion system the amplitude of the evoked response is virtually abolished.

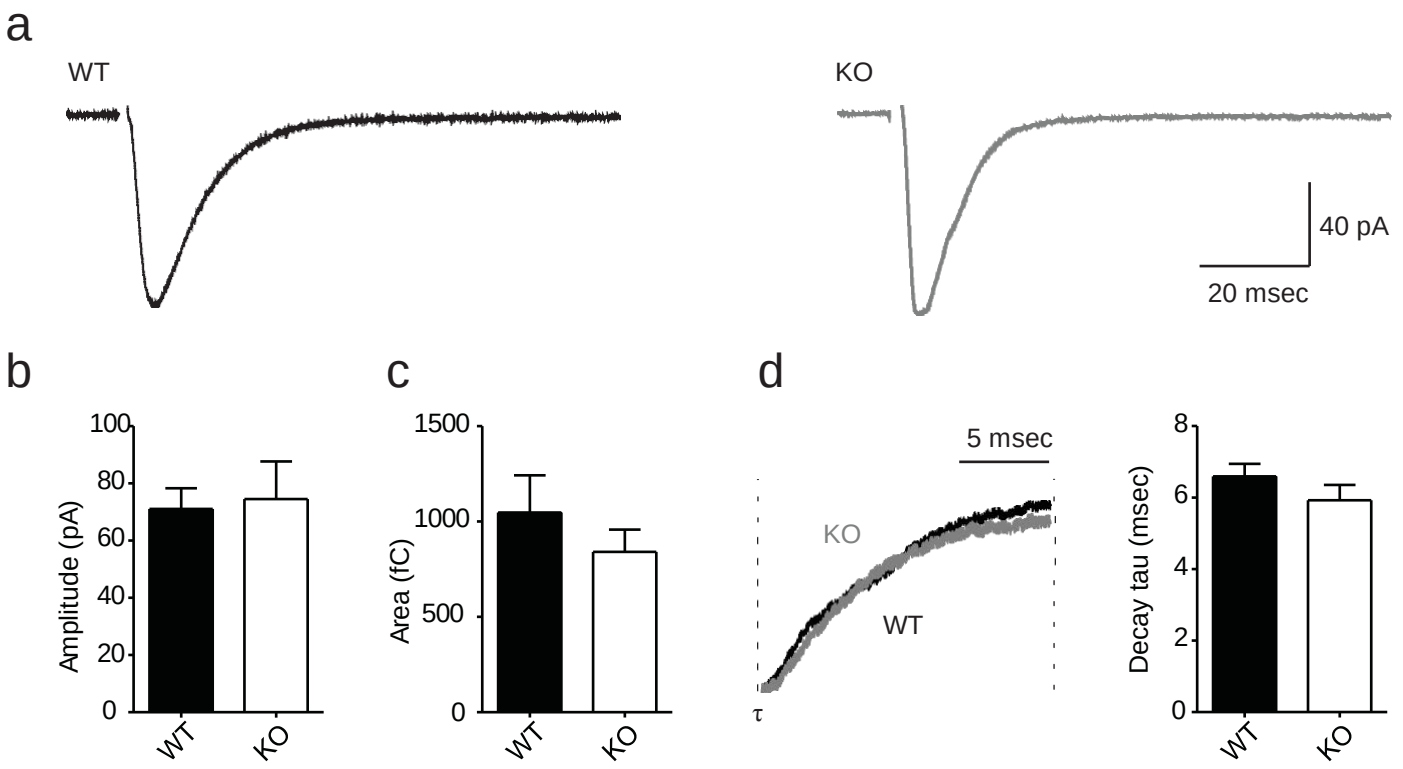

Supplementary Figure S2. SYN2 deletion does not induce changes in the basal excitatory synaptic transmission.

a. Representative traces of eEPSC recordings from WT and KO dentate gyrus granule neurons. **b.** Histogram of the mean (± sem) amplitude of eEPSCs for WT and KO neurons (71.1 ± 7.2 pA, n = 13 neurons/5 mice and 74.5 ± 13.1, n = 10 neurons/3 mice for WT and KO, respectively; p = 0.808). **c.** Histogram of the mean (± sem) charge of eEPSCs for WT and KO neurons (1047 ± 195 and 841 ± 116 fC for WT and KO, respectively; p = 0.411). **d.** Representative deactivation traces for the decay of WT (black trace) and KO eEPSC (gray trace). A monoexponential function was used for fitting the EPSC kinetics and the resulting mean (± sem) τ values are shown in the histogram (6.59 ± 0.35 and 5.92 ± 0.43 ms for WT and KO, respectively; p = 0.235). A two-tailed unpaired Student's *t* test was used for the statistical analysis in all cases.

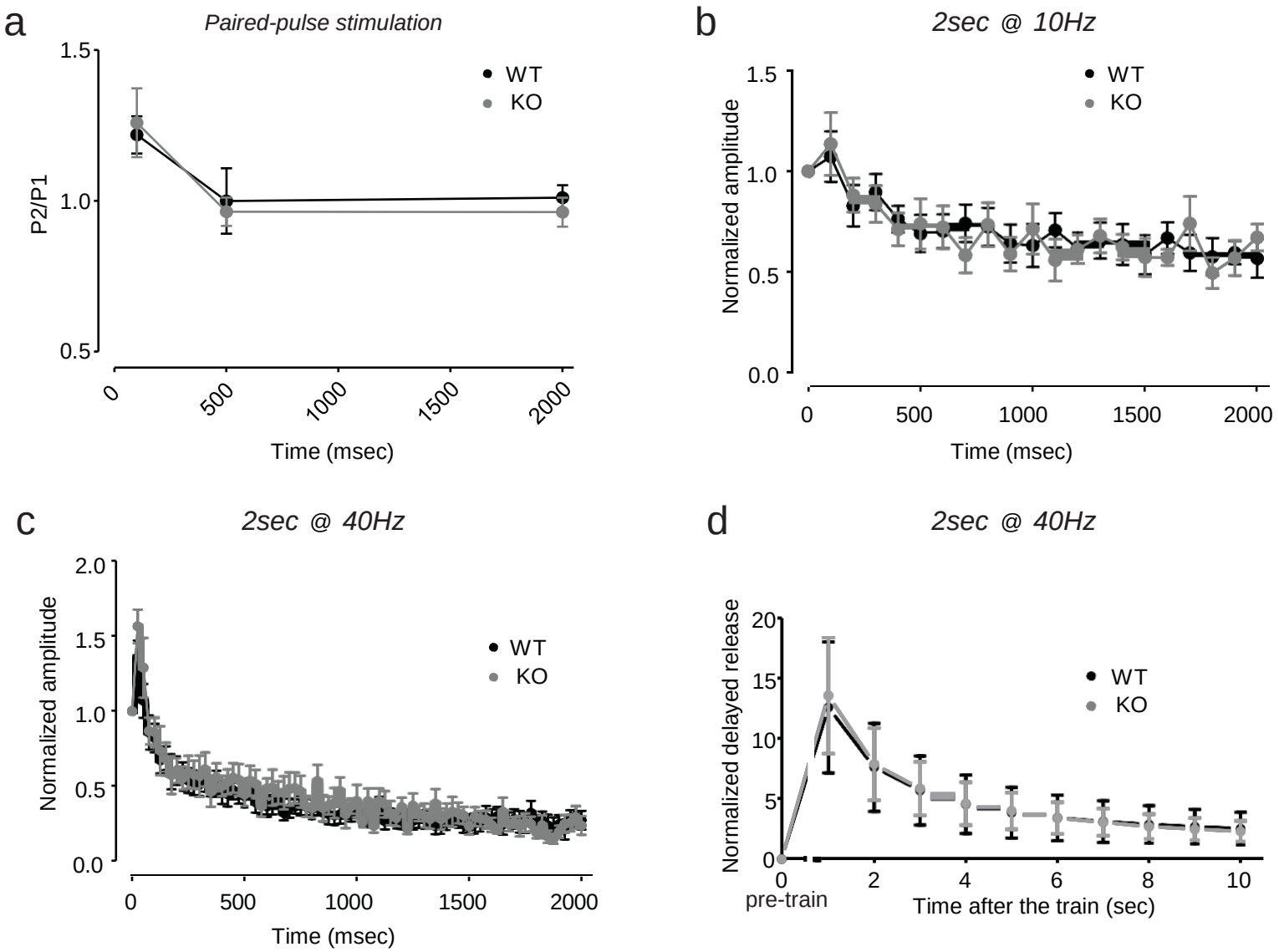

Supplementary Figure S3. SYN2 deletion does not induce changes in short-term plasticity or delayed asynchronous release at excitatory synapses.

a. Paired pulse facilitation (PPF) at excitatory synapses was recorded from WT (black) and KO (gray) dentate gyrus neurons in response to paired stimulation of the medial perforant path at the indicated inter-stimulus intervals (ISIs). The mean (± sem) PPF observed in WT (black symbols; n = 12 neurons/5mice) and KO (gray symbols; n = 8 neurons/3mice) neurons is plotted as a function of the ISI. **b,c.** Plots of normalized peak amplitude (means ± sem) versus time showing the multiple-pulse depression of the excitatory response evoked by stimulation of the medial perforant path for 2 sec at 10 Hz (**b**) and 40 Hz (**c**) in WT (black) and KO (gray) neurons. **d.** Plot of the mean (± sem) charge of the delayed asynchronous release at excitatory synapses of the dentate gyrus as a function of time after the end of the stimulation train. Data (black and gray symbols/lines for WT and KO, respectively) were normalized to the pre-train spontaneous release.

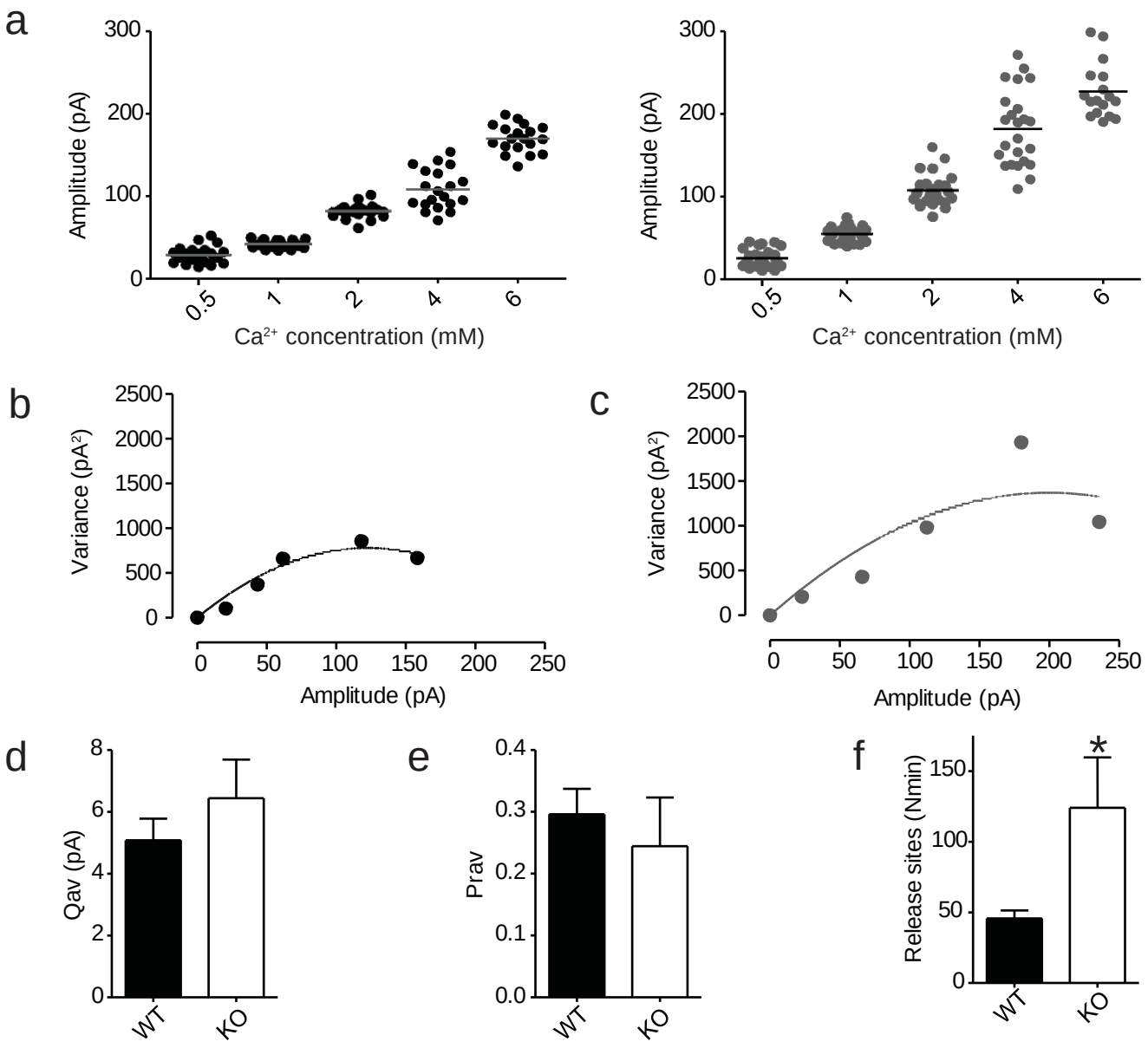

Supplementary Figure S4. Estimation of the quantal parameters of inhibitory synaptic transmission in WT and Syn II KO neurons

a. Plots of eIPSCs amplitude analyzed at various levels of release probability obtained by varying the external Ca^{2+} concentration (0.5, 1, 2, 4, 6 mM) in representative WT (left; black dots) and Syn II KO (black; gray dots) granule neurons. The horizontal lines show the mean amplitude during each epoch. **b,c**. The variance in eIPSC amplitude is plotted against the mean amplitude for each epoch and fitted with a parabola to estimate the release probability (Pr_{av}), the average quantal size (Q_{av}) and the mean number of release sites (N_{min}) (*see Supplementary Methods*) in representative WT (**b**) and KO (**c**) synapses. **d-f.** Histograms of the mean (± sem) Q_{av} (d), Pr_{av} (e) and N_{min} (f) (n = 9 neurons/6mice and n = 9 neurons/5mice for WT and KO, respectively).* p = 0.034, two-tailed unpaired Student's *t* test.

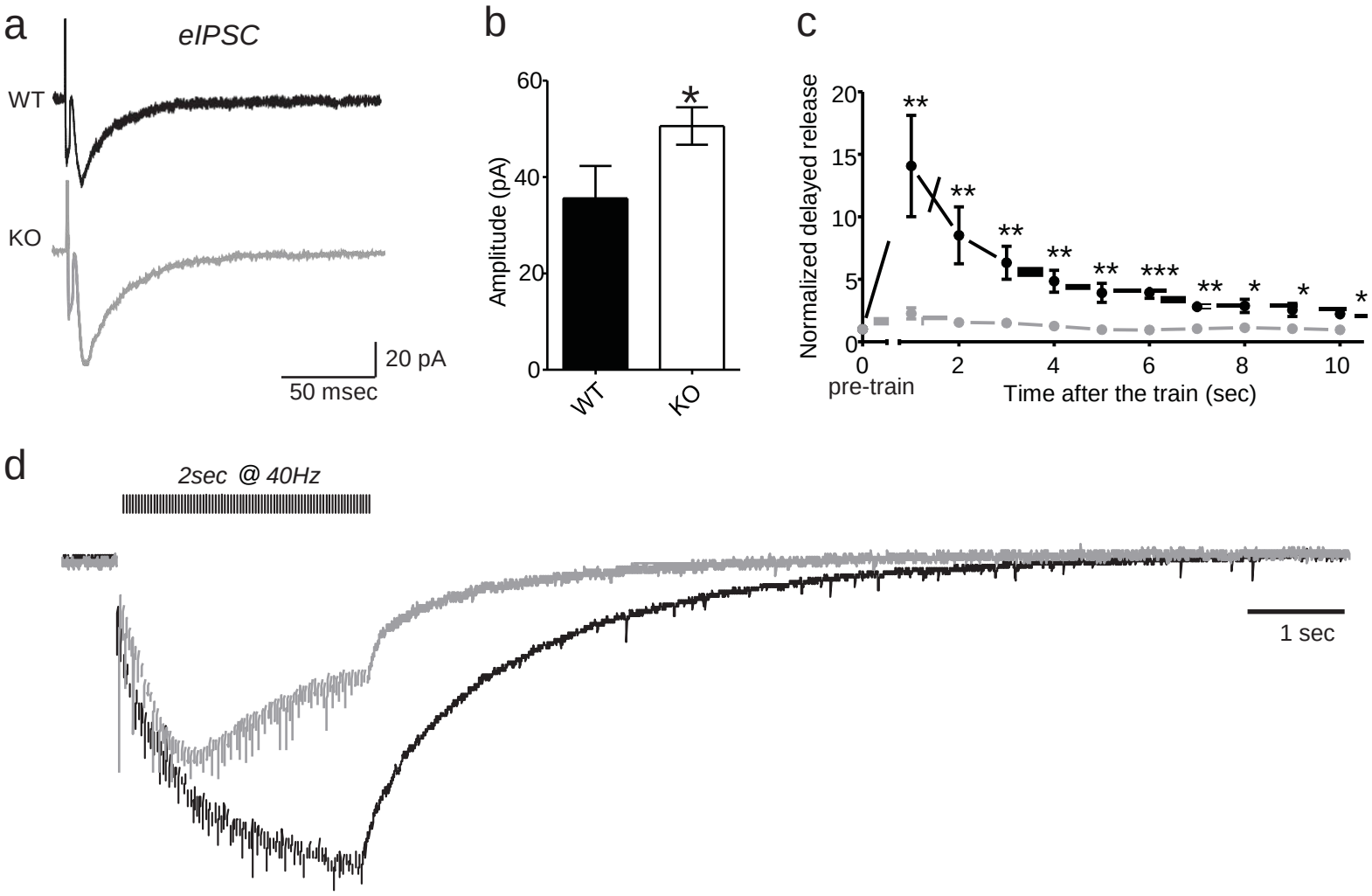

Supplementary Figure S5. Increased synchronous and decreased asynchronous GABA release in inhibitory synapses of adult Syn II KO dentate gyrus.

Experiments were performed in 4- to 8-months old mice. **a.** After blocking glutamatergic transmission with 50 µM D-APV and 10 µM CNQX, we employed minimal extracellular stimulation of the medial perforant path to elicit monosynaptic inhibitory responses in WT and KO adult dentate gyrus granule neurons **a.** Representative traces are shown for WT (black) and KO (grey) neurons. **b.** Histogram of the mean (± sem) amplitude of eIPSCs in WT slices (34.43 ± 7.60, n = 6 neurons/3 mice) and KO slices (58.19 ± 5.36 pA, *n* = 12 neurons/7mice; p = 0.026; two-tailed unpaired Student's *t* test) **c.** Representative traces of the inhibitory delayed asynchronous response in adult WT (black) and KO (gray) dentate gyrus granule cells after stimulation of the medial perforant path. **d.** Plot of the mean (± sem) charge of the delayed GABA release as a function of time after the end of the stimulation train. Data (black and gray symbols/lines for WT and KO, respectively) were normalized to the pre-train spontaneous release. *p<0.05, **p<0.01 and ***p<0.001, Welch's *t* test. n=15 and n=22 neurons from WT (4 mice) and KO (8 mice), respectively.

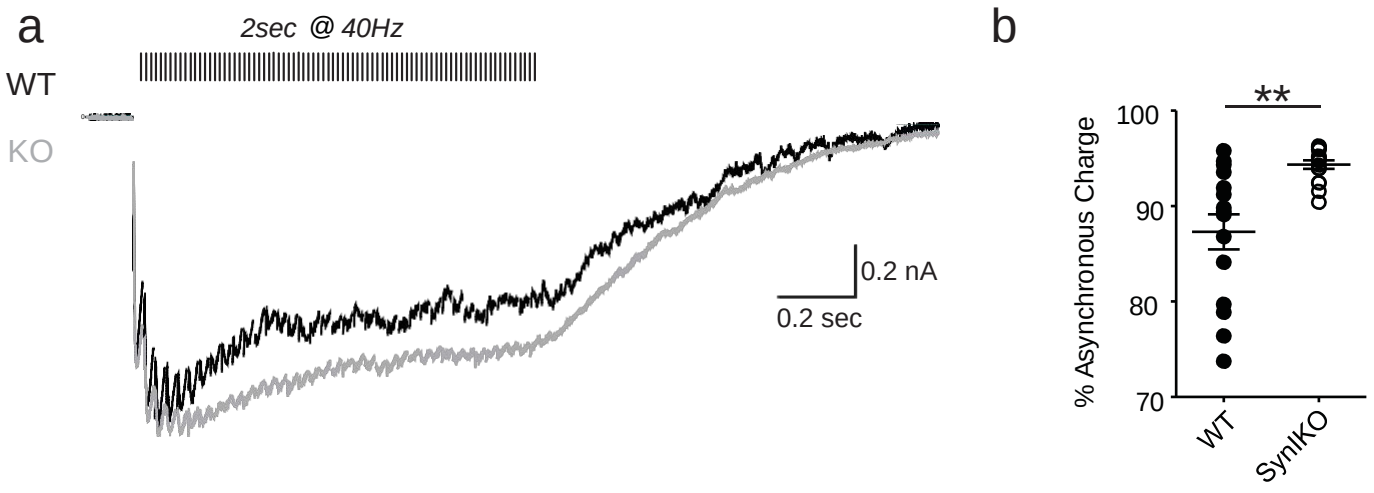

Supplementary Figure S6. Increased asynchronous inhibitory release in Syn I KO neurons.

a. Representative traces of the inhibitory responses to a train of 1 sec at 40 Hz in hippocampal primary neuronal cultures. Note the increased asynchronous inhibitory response in Syn I KO neurons (gray) with respect to the WT (black). **b.** Mean (± sem) percentage of the asynchronous inhibitory release induced by the stimulation with respect to the total response (see Supplementary Methods) (87.26 ± 1.8 %, n =15 neurons for WT and 94.31 ± 0.4 %, n = 16 neurons for KO p = 0.002, Welch's *t* test).

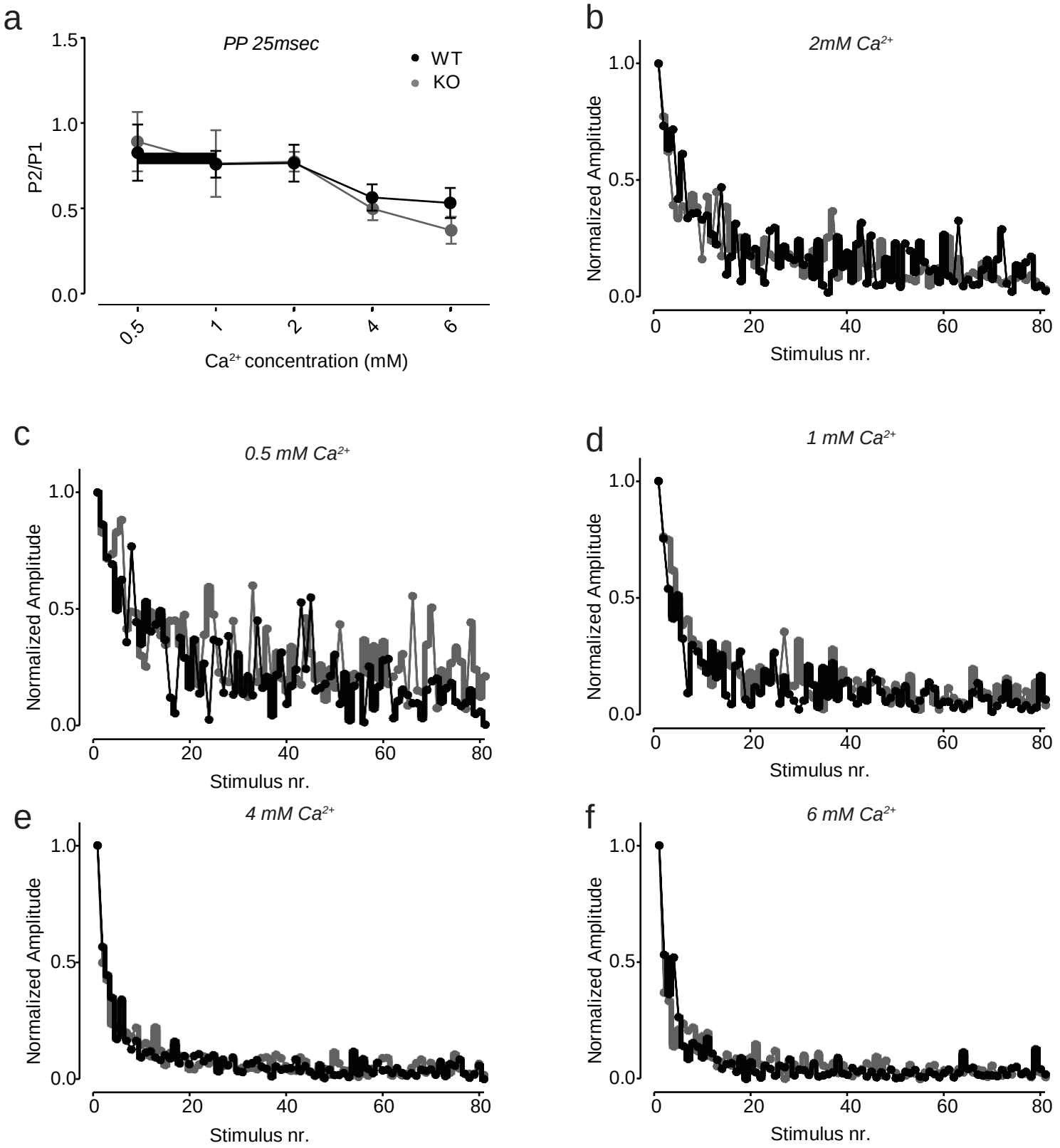

Supplementary Figure S7. Changes in the extracellular Ca^{2+} concentration do not affect the short-term plasticity of inhibitory synapses in Syn II KO mice.

a. Paired pulse depression (± sem) at inhibitory granule synapses was recorded from WT (black) and KO (gray) neurons as the ratio (P2/P1) between the first two responses form a train at 40 Hz (ISI: 25 ms) at different Ca^{2+} concentrations. **b-f.** Normalized depression of IPSCs in response to a train of 2 sec at 40 Hz in WT (black) and KO (gray) neurons at various Ca^{2+} concentrations. n = 9 neurons/6 mice for WT and 8 neurons/5 mice for Syn II KO.

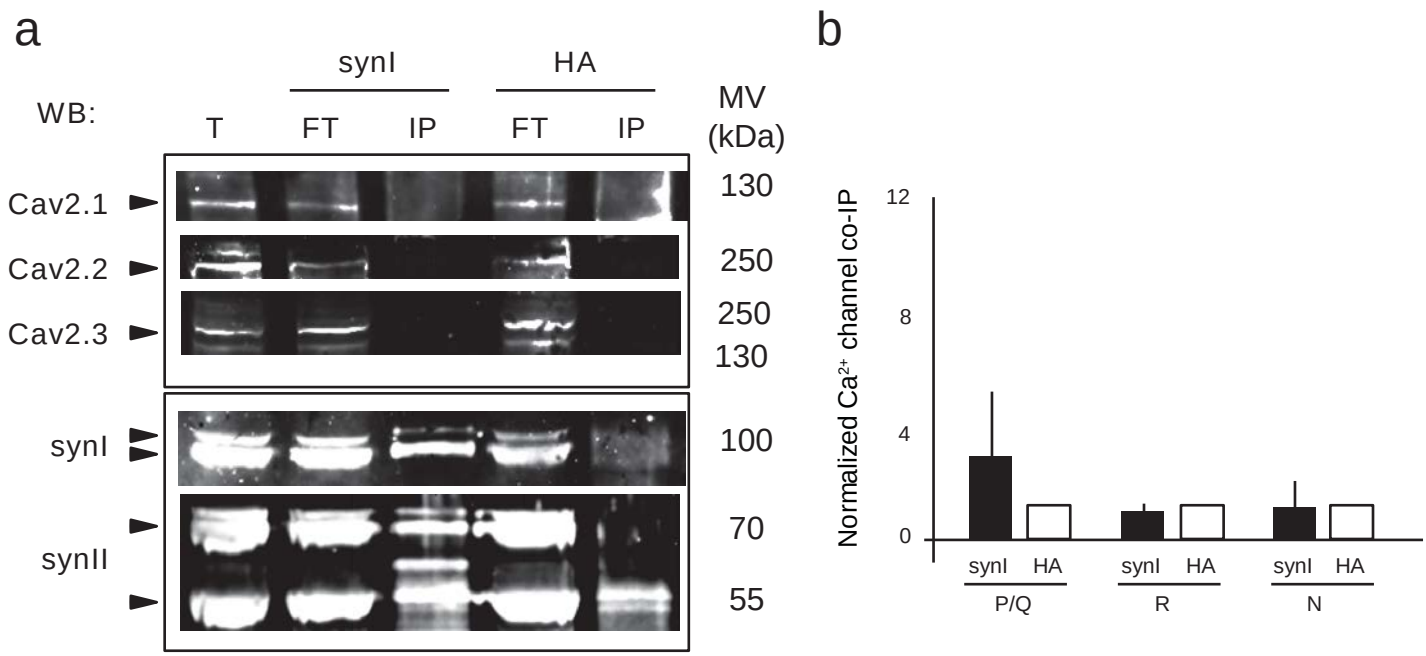

Supplementary Figure S8. Syn I does not interact with presynaptic Ca^{2+}-channels. Cortical neuron lysates were immunoprecipitated with anti-SynI antibodies or anti-HA antibodies, as indicated. After electrophoretic separation of the immunocomplexes, membranes were probed with antibodies specific for anti-Cav2.1 (P/Q-type), anti-Cav2.2 (N-type) and anti-Cav2.3 (R-type) Ca^{2+} channel subunits, as indicated. **a.** A representative immunoblot is shown. **b.** Quantification of the co-immunoprecipiated immunoreactive signal for Ca^{2+} channel subunits, normalized to the binding to the HA control, (mean ± sem, n=3 independent experiments, *right panel*). T, 100 mg of total lysate before immunoprecipitation; FT, 100 mg of flow-through after immunoprecipitation; IP, immunoprecipitated material.

Methods

Electron microscopy

Acute slices were fixed by immersion in 1.3% glutaraldehyde in 66 mM sodium cacodylate buffer, post-fixed with 1% OsO_4 in 1,5% $K_4Fe(CN)_6$ and 0.1 M sodium cacodylate, *en bloc* stained with 0.5% uranyl acetate, dehydrated through a series of graded ethanol, washed in propylene oxide and flat embedded in Embed 812 between two Aclar sheets. After 48 h of polymerization at 60°C, selected regions of the slices containing molecular layer of the dentate gyrus were excised, glued on blocks of resin and cut in a Leica EM UC6 ultramicrotome. Ultrathin sections (70-90 nm) were collected on formvar carbon coated nickel grids and processed for GABA immunolabeling as previously described[61]. After 5 min incubation in TBST 7.6 (Tris HCl 0.05 M, pH 7.6, with 0.9% NaCl and 0.1% Triton X-100), grids were incubated with rabbit antiserum against GABA (Sigma A2052, 1:10.000 in TBST) overnight in a moist chamber at RT. Grids were then washed twice for 5 min and once for 30 min in TBST 7.6. After 5 min of conditioning in TBST 8.2 (0.05 M Tris, pH 8.2, with 0.9% NaCl and 0.1% Triton X-lO0), grids were incubated for 2 h in goat anti-rabbit IgG conjugated to 10 nm colloidal gold (Aurion, Netherlands) diluted 1:25 in TBST 8.2. They were then washed twice in TBST pH 7.6, rinsed in deionized water, allowed to air-dry and counterstained with 1% uranyl acetate and Sato's lead citrate. Grids were observed in a JEOL JEM-1011 microscope operating at 100 kV. Images of GABA-immunopositive synaptic terminals making contact with granule cell dendrites were taken at a magnification of 12.000x using an ORIUS SC1000 CCD camera (Gatan Inc., Pleasanton, CA). Images were analyzed with ImageJ by measuring the following

parameters: cross-sectional synaptic area (areas occupied by mitochondria were excluded), SV number, active zone length, and docked vesicles.

Multiple probability fluctuation analysis.

The analysis of the three main determinants of synaptic function, namely the average amplitude of the postsynaptic response to a neurotransmitter quantum (Q_{av}), the average probability of release one SV from a release site (Pr_{av}), and the number of independent release sites (N), was performed by building variance–mean (V–M) plots[17,62]. Q_{av}, Pr_{av}, and N were derived from the parabolic relationship between eIPSC variance and mean postsynaptic current amplitude (I_{av}) as follows:

$$V = A\, I_{av} - B\, I_{av}^2$$

recorded under different release probability conditions by assuming that:

$$I_{av} = N * Q_{av} * Pr_{av}$$ [63-64]

The free parameters A (initial slope) and B (curvature of the parabola) were iteratively adjusted to optimally fit the V–M plots and used to calculate a weighted mean of Pr_{av} and Q_{av} and a lower limit for the number of independent release sites, N_{min}:

$$Pr_{av} = I_{av} * (B/A)\ (1 + CV_i^2)$$

$$Q_{av} = A / (1 + CV_i^2)$$

$$N_{min} = 1 / B,$$

where CV_i is the coefficient of variation of mIPSC amplitudes at an individual release site. In our case, CV_i was 0.32 ± 0.02 and 0.35 ± 0.03 in WT and KO neurons,

respectively. The probability of release was varied by changing the concentrations of Ca^{2+} in the perfusion system (0.5, 1, 2, 4, 6 mM). I_{av} and V were calculated over a stable epoch of 30 events after the exchange of each Ca^{2+} concentration. A zero point was included in each V–M plots to indicate that the noise variance was subtracted.

Electrophysiology of primary neuronal cultures

Syn I KO mice were generated by homologous recombination[65]. Offspring of littermates of WT and homozygous Syn I KO mice were used throughout. All experiments were carried out in accordance with the guidelines established by the European Community Council (Directive 2010/63/EU of September 22nd, 2010) and were approved by the Italian Ministry of Health. Mice were killed by inhalation of CO_2, and embryonic day 17 (E17) embryos were removed immediately by cesarean section. Removal and dissection of hippocampus, isolation of neurons and culturing procedures were as previously described[17].The isolated hippocampal neurons were plated at low density (100 cells/mm^2) and maintained in a culture medium consisting of Neurobasal, B-27 (1:50 v/v), glutamine (1% w/v), penicillin-streptomycin 1% (all from Invitrogen, Carlsbad, CA). Every 7 d for 3–4 weeks, a half-volume medium replacement was performed. Electrophysiological experiments were performed on 7–28 days in vitro (DIV) neurons.

Patch electrodes, fabricated from thick borosilicate glasses (Hilgenberg, Mansfield, Germany), were pulled and fire-polished to a final resistance of 3–4 MΩ. Monosynaptic GABAergic IPSCs were investigated either in pairs of monosynaptically connected neurons of 7–28 DIV. Whole-cell patch-clamp recordings from presynaptic and postsynaptic neurons were simultaneously performed using an EPC-10 double amplifier

(HEKA Elektronic, Lambrecht, Germany). Current pulses of 0.1/0.3 msec and variable amplitude (10–45 µA) delivered by an isolated pulse stimulator (model 2100; A-M Systems, Carlsburg, WA) were required to induce trains of eIPSCs with short latency (2–4 msec). Data were acquired at 5–20 kHz sample frequency and filtered at half the acquisition rate with an 8-pole low-pass Bessel filter. Recordings with leak currents > 100 pA or series resistance > 20 MΩ were discarded. Data acquisition was performed using PatchMaster programs (HEKA Elektronic) and analysed using Clampfit (Molecular Devices, Sunnyvale CA). All the experiments were performed at room temperature (22–24°C). Trains of 1 sec at 40 Hz of eIPSCs were recorded in extracellular solution (Tyrode solution) containing (in mM): 2 $CaCl_2$, 140 NaCl, 1 $MgCl_2$, 10 HEPES, 4 KCl, 10 glucose and pH 7.3. D-AP5 (50 µM), CNQX (10 µM) and CGP58845 (5 µM) were added to block NMDA, non-NMDA, and $GABA_B$ receptors, respectively. Asynchronous release was evaluated, for each response in train, as the difference between the total transferred charge and the synchronous charge. The synchronous charge component of each response was calculated as the integral of the current with respect to an individual baseline determined 2 msec before each stimulus[3, 48], using a proprietary program developed in an R-CRAN environment (T. Nieus, unpublished data). The total release during the train was calculated using cumulative charge analysis in the same way of cumulative amplitude analysis, to include in the analysis both synchronous and asynchronous release components[33].

Supplementary References

61. Phend, K.D., Weinberg, R.J. & Rustioni, A. Techniques to optimize post-embedding single and double staining for amino acid neurotransmitters. *J Histochem Cytochem* **40**, 1011-1020 (1992).

62. Clements, J.D. & Silver, R.A. Unveiling synaptic plasticity: a new graphical and analytical approach. *Trends Neurosci* **23**, 105-113 (2000).

63. Reid, C.A. & Clements, J.D. Postsynaptic expression of long-term potentiation in the rat dentate gyrus demonstrated by variance-mean analysis. *J Physiol* **518 (Pt 1)**, 121-130 (1999).

64. Silver, R.A., Momiyama, A. & Cull-Candy, S.G. Locus of frequency-dependent depression identified with multiple-probability fluctuation analysis at rat climbing fibre-Purkinje cell synapses. *J Physiol* **510 (Pt 3)**, 881-902 (1998).

65. Chin, L.S., Li, L., Ferreira, A., Kosik, K.S. & Greengard, P. Impairment of axonal development and of synaptogenesis in hippocampal neurons of synapsin I-deficient mice. *Proc Natl Acad Sci U S A* **92**, 9230-9234 (1995).